Available online at www.sciencedirect.com
ScienceDirect
Ceramics International 33 (2007) 1435–1443
CERAMICS INTERNATIONAL
www.elsevier.com/locate/ceramint

Elaboration and characterization of a refractory based on Algerian kaolin

M. Kolli [a], M. Hamidouche [a], G. Fantozzi [b,*], J. Chevalier [b]

[a] *Laboratoire des Matériaux Non Métalliques (LMNM), dépt OMP, Faculté des Sciences de l'Ingénieur, Université Farhat Abbas, Sétif 19000, Algeria*
[b] *GEMPPM, UMR CNRS 5510, Bat. Blaise Pascal, INSA, 20 Avenue Albert Einstein, Villeurbanne 69621, France*

Received 20 February 2006; received in revised form 3 June 2006; accepted 4 June 2006
Available online 18 January 2007

Abstract

A refractory material was elaborated from kaolin extracted from the region of Djebel Debbagh (Algeria). Kaolin grog was obtained by calcination at a temperature of 1350 °C during 1 h. It was used as aggregates with granulometric distribution composed of fine fraction (mean grain size: 100–250 μm) and coarse fraction (mean grain size: 1000–2500 μm). Crude kaolin (size < 75 μm) was also used as a binder with an amount representing 15% of the dry material. After a 9.28% moistening and a rotting of 1 day, cylindrical samples were shaped by uniaxial pressure at 80 MPa. The samples were submitted to a natural drying during 24 h, a stoving at 100 °C and a calcination at 600 °C during 1 h. They were fired at high temperatures between 1250 and 1450 °C.

An X-ray diffraction (XRD) analysis showed that the refractory samples are composed of mullite and silica. Silica is a mixture of a vitreous phase and cristobalite at 1300, 1350 and 1400 °C and becomes completely amorphous when the samples are fired at higher temperature (1450 °C). The sample porosity is about 30%. The mechanical tests carried out as a function of temperature revealed different behaviours of the material. From the ambient up to 600 °C, the refractory behaviour is pseudo-plastic caused by micro-cracking. Between 700 and 900 °C, the samples become more rigid. At 1000 °C, the material exhibits a visco-plastic behaviour. The amorphous phase governs the sample properties variation with temperature increasing. Its content varies between 28% and 34% according to the firing temperature. Thermal shock tests realized in water showed that the refractory samples present good thermal shock resistance.

Keywords: D. Mullite; Refractory materials; Kaolin; Amorphous phase

1. Introduction

Industrial refractory materials are currently made from natural raw or synthesized components consisting essentially of metallic oxides. Most of these materials are part of the alumina–silica system [1,2]. The alumina–silica range of refractories is the largest of refractory groups, in terms both of the number of varieties and in its share of the total refractory market [3–5].

Kaolinitic clays are used to make fire-clays and silica-clays refractory materials. Alumina–silica (cyanide, sillimanite and andalousite) and alumina hydrates (boehmite, diaspore, gibbsite) are the main raw materials for the alumina refractory products. Silica in a form of quartzite, sand or aggregates is used for the silica based refractory materials elaboration [6]. Kaolin has the advantage to be easily accessible and not expensive in natural open work seams [1,7]. The main mineral constituent of the kaolin is the kaolinite. Its theoretical formula $[Si_2Al_2O_5(OH)_4]$ is most often presented in the form: $Al_2O_3{\cdot}2SiO_2{\cdot}2H_2O$. The kaolinite is a phyllosilicate composed of a silica tetrahedral layer $[Si_2O_5]^{2-}$ and an octahedral hydroxide layer $[Al_2(OH)_4]^{2+}$.

Kaolinite firing induces numerous complex structural and microstructural transformations leading to the formation of mullite and a silica phase, mainly in a vitreous form, according to the following reaction [8,9]:

$$3(Al_2O_3{\cdot}2SiO_2{\cdot}2H_2O) \rightarrow 3Al_2O_3{\cdot}2SiO_2 + 4SiO_2 + 6H_2O$$

Mullite phase is characterized by some advantageous properties at high temperatures [10]. It presents a good corrosion

* Corresponding author.
E-mail address: gilbert.fantozzi@insa-lyon.fr (G. Fantozzi).

0272-8842/$32.00
doi:10.1016/j.ceramint.2006.06.009

resistance, a low-dilatation coefficient and thermal conductivity, a good creep and thermal shock resistances. These advantages confer to this phase different refractory applications [11–13].

In the refractory products manufacturing (shaped, monolithic or electrofused), different processes can be used. Shaping and firing techniques are the most used. Different shaping methods can be chosen according to the sought properties and the cost of the finished products. Security and environment restrictions are also not negligible factors to consider [14]. After determining the constituent's quantity and mixing the raw materials (calcined grog) and crude kaolin (binder), the products can be shaped by dry pressing in order to obtain good refractory properties [1,3,15,16]. The refractory drying before firing does not take much time. This makes the refractory manufacturing process relatively fast. Besides, a mass production is possible [15,16]. The degreasing grog (chamotte) content is more important than the plastic matter (crude clay) in the shaping process by dry pressing. The chamotte brings to the mixture, the mineralogical elements already transformed (mullite, cristobalite) leading to a better volume stability during firing. It furthermore constitutes the refractory skeleton in the samples with the crushed crude clay playing the role of a binder. It enables also the ceramic bond formation and limits the shrinkage and the cracking of the clay during drying and firing. Firing is the most important step since it gives to the product its final physical characteristics (densification, mechanical strength, durability and refractoriness) and its mineralogical structure (chemical modification of components, grain growth, etc.) [3,17,18].

The thermo-mechanical behaviour of alumina–silica refractory materials is governed by the vitreous phase. The glassy phase has at least two potentially beneficial effects on the thermal shock resistance. First, the vitreous phase allows the thermal/residual stresses to accommodate or relax during up quenching or down quenching. Second, it can be used to promote crack-tip shielding by bridging cracks under thermal cycling conditions. This results in a decrease in the crack-driving forces and therefore improves the brick life [19]. However, the mechanical behaviour at high temperatures is considerably affected. The vitreous phase is responsible for the limitation of the refractory use at high temperatures [10]. In these conditions, creep phenomenon is more pronounced [1]. The quantification of this vitreous phase becomes necessary.

The selective dissolution in fluorhydric acid is a simple and frequently used technique for quantifying the silica amorphous phase. Besides the minor inconvenience of the residues harmfulness encountered with this technique, it is easily experimented and gives acceptable results. The principle consists of estimating the dissolution kinetics in an aqueous solution of fluorhydric acid. The amorphous dissolution rate is more rapid than that of the crystalline phases [20,21]. Vitreous silica, with a relatively opened structure, dissolves faster than silica quartz. The dissolution reaction is:

$$SiO_2 + 6HF \rightarrow SiF_6H_2 + 2H_2O$$

The silica–HF reaction can also result into the tetrafluorosilicate gas SiF_4 produced according to the following reaction:

$$SiO_2 + 4HF \rightarrow SiF_4 + 2H_2O$$

If a product, made of a mixture of amorphous and crystalline phases (alumina–silica for example) is attacked by an HF acid for various durations, the dissolution variation curve presents two distinct slopes. The first slope represents the superposed dissolutions of the two phases. The second weaker slope, starting after a complete dissolution of the amorphous phase, corresponds exclusively to the crystalline phase dissolution. An extrapolation of the second linear part toward the starting time ($t = 0$) allows the determination of the vitreous phase content.

The infrared (IR) spectroscopy is a method frequently used to study the clays structures, bonding and chemical properties of ceramics [22,23]. The vitreous silica pattern presents several peaks characterizing the Si–O bond. The intensity of these peaks allows to estimate its evolution in ceramics during firing.

In addition to their use at high temperatures, refractory materials can be subject to sudden temperature variations [19]. These thermal shocks are generally sub-critical but cyclically repeated. The repeated brutal temperature drops can lead to the refractory deterioration. Several authors [24,25] elaborated different theories for preventing brittle materials from thermal shock deterioration. Ceramics with a high mechanical strength can resist to cracking initiation. However, once a crack is initiated under critical thermal stresses, its propagation is catastrophic. On the other hand, if the cracking occurs at moderate stresses, the material damaging by micro-cracking reduces the mechanical strength after the thermal shock at an acceptable level.

2. Experimental procedure

In this work, we used a kaolin extracted from Djebel Debbagh (north-east of Algeria) designated DD3. Its chemical composition with its fire mass loss are indicated in Table 1. We can observe that it contains nearly the same content of silica (39.87%) and alumina (38.36%).

Table 1
Chemical composition and calcination losses of DD3 kaolin [26]

Oxides	Mass%
SiO_2	39.87
Al_2O_3	38.36
Fe_2O_3	1.14
CaO	0.78
Na_2O	0.48
MnO	0.46
SO_3	0.45
MgO	0.24
K_2O	0.20
P_2O_5	0.02
TiO_2	0.02
Cr_2O_3	0.01
Calc. loss	17.27
Total	99.69

In a previous study [8], it was shown that this kaolin undergoes several microstructural transformations during firing. Up to 600 °C, we noticed an important shrinkage and mass loss, probably due to the moisture extraction, to the organic impurities combustion and the structural water evaporation. Above 980 °C, there is a formation of mullite, of γ-alumina and a glassy phase as mentioned in Ref. [8]. At temperatures higher than 1200 °C, the last two phases react and form a secondary mullite. Above 1400 °C, the obtained product contains exclusively mullite and a glassy phase of complex composition.

The elaboration steps of the samples are shown in the flow chart presented in Fig. 1. The tests conditions were optimised in a previous work [26]. We used as grog (chamotte) the DD3 kaolin fired industrially at 1350 °C. It mainly consists of mullite and cristobalite. We used a discontinuous granulometry, composed of a fine fraction (grain size range: 100–250 μm) and a coarse fraction (grain size range: 1000–2500 μm). A mixture containing 40% of fine fraction and 60% of coarse fraction was prepared. In order to assure a good firmness of the green samples during shaping, we used crude DD3 kaolin as a binder. This last consist of fine powder (<75 μm) and it represents 15% of the total mixture mass. After moistening (adding a 9.28% water mass) and a rotting during 24 h inside hermetic bags, the samples shaping was made by uniaxial compaction with a pressure of 80 MPa. The samples have a cylindrical form of 30 mm diameter and 50 mm height. The green samples were dried and fired during 1 h at 600 °C at a slow heating rate (1 °C/min). The firing was made at temperatures between 1250 and 1450 °C for 1 h.

The different phases formed after firing were identified by X-ray diffraction. A Geigerglex diffractometer Cu Kα type (Rigaku) with λ = 1.541 Å was used.

Samples were prepared by the KBr pellets technique and analysed by FT-IR in a transmission mode. The pellets making was done by pressuring the KBr containing 1% of the material powder whose mean grains size is less than 125 μm. All spectra were obtained with a resolution of 2 cm^{-1} and 15 scans.

Apparent density was measured by Archimedes's method and the absolute density by using an automatic helium pycnometer (ACCUPYC 1300). The samples were kept in a stove at a temperature of 60 °C during at least 24 h.

Mechanical tests were made on a MTS type machine equipped with a kiln for high temperature tests. The test temperatures were performed between ambient and 1000 °C. At ambient temperature, both the axial compression and the indirect tension test (Brazilian test) were applied. The loading–displacement curves were systematically derived for every test. The strengths in both the compression and the Brazilian test were, respectively, determined by the following equations:

$$\sigma_C = \frac{4F}{\pi D^2} \quad \text{(compression)}$$

$$\sigma_T = \frac{2F}{\pi D h} \quad \text{(Brazilian test)}$$

where F is the applied load, D is the sample diameter and h is the height.

Static elastic modulus (Young's modulus) was evaluated from these tests using Hooke's law. On prismatic samples (cut from cylinders), we also calculated the dynamic elastic

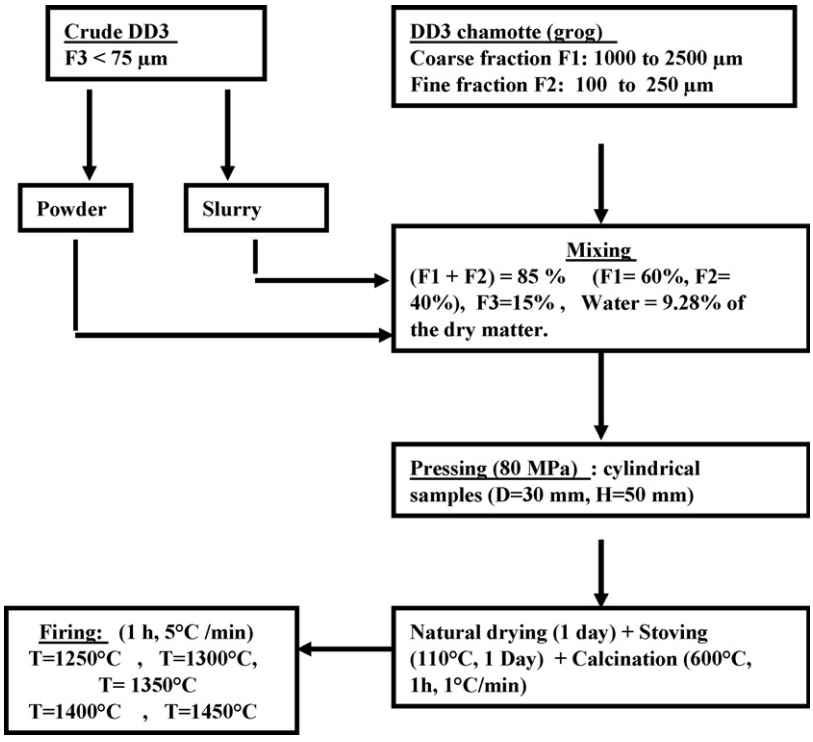

Fig. 1. Refractory elaboration flow chart.

modulus after measurement of resonance frequencies using a ''Grindo Sonic'' apparatus.

After the mechanical tests, some samples fragments were crunched and sifted to a mean grains size less than 125 μm in order to quantify the vitreous phase. The test was done by chemical attack with 2% hydrofluoric acid solution (1.13 mol/l). The mass loss was measured for different dissolution periods. A powder sample of 10 g was put in 250 ml of HF solution. We established the dissolution kinetic of the powder (mass loss versus attack duration) in order to deduce the amorphous phase rate.

Two types of thermal shock tests were used: the first one is used with various temperature differences and the second is submitted to cyclic variations at the same temperature difference. Only samples fired at 1350 °C were tested. For the first case, we heated six samples at the same time during 15 min at different temperatures: 750, 850, 950 and 1050 °C. Then, the samples are plunged into cooling water maintained at 25 °C. After drying, mechanical strengths (indirect traction and compression) are determined. The cyclic thermal shock tests were done according to the DIN 51 068 normalization [27]. The samples were heated during 15 min at 950 °C, and immediately immersed in the cooling water at 25 °C during 3 min. After drying during 2 h at 110 °C, the test is repeated until the samples break into several fragments.

3. Results and discussion

The refractory samples shaped by dry pressing and fired during 1 h at different temperatures (1300, 1350, 1400 and 1450 °C) were analysed by X-ray diffraction (XRD). The obtained spectra are shown in Fig. 2.

The results reveal that elaborated refractories contain mullite (JCPDS 15-0776 index-card) and silica. The developed mullite has a needle shape and is oriented in all directions as shown in Fig. 3. This microstructure shows the presence of mullite with an important amount of amorphous phase. Silica excess in the chamotte (grog) and the binder (crude kaolin)

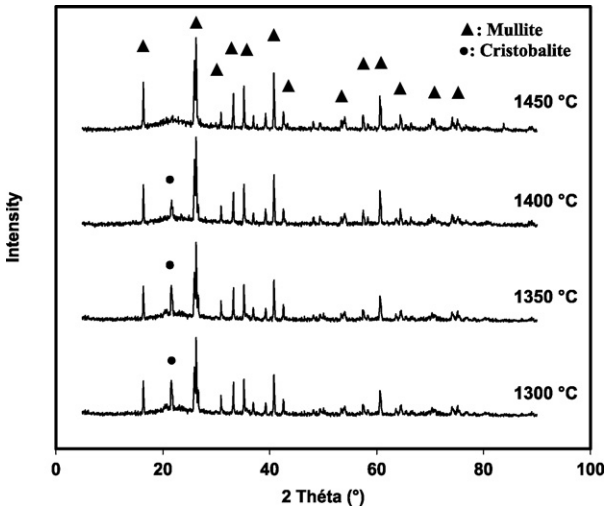

Fig. 2. XRD patterns of samples fired at different temperatures.

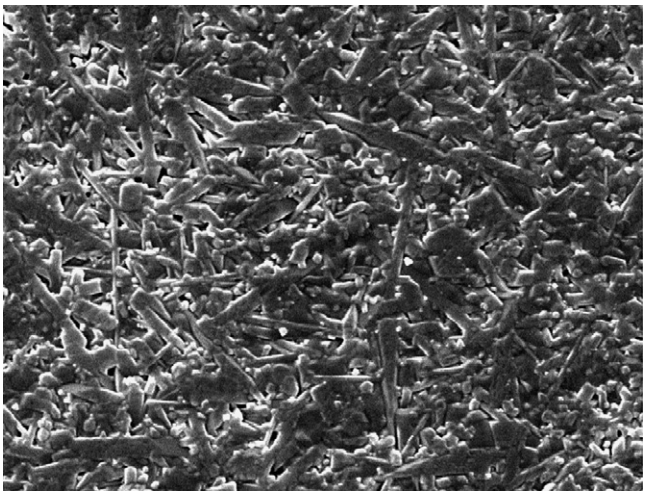

Fig. 3. SEM microstructure of polished and thermally etched section (1300 °C for 1 h) of DD3 kaolin specimen fired at 1400 °C during 1 h (5000×).

takes different phase forms. It takes a cristobalite form (JCPDS 27-0605) at 1300 and 1350 °C, and becomes totally amorphous after firing at 1450 °C. The cristobalite transformation takes place gradually. We can notice from X-ray spectrum made at 1400 °C (Fig. 2) that the cristobalite intensity peak ($2\theta = 21.6°$) diminishes when the firing temperature increases.

FT-IR spectra obtained for samples fired at 1250 and 1450 °C are shown in Fig. 4. These patterns present several absorption bands. Each of them corresponds to vibration of a functional group. For example, the large band observed in the vicinity of 3445 cm^{-1} represents the OH stretching band of

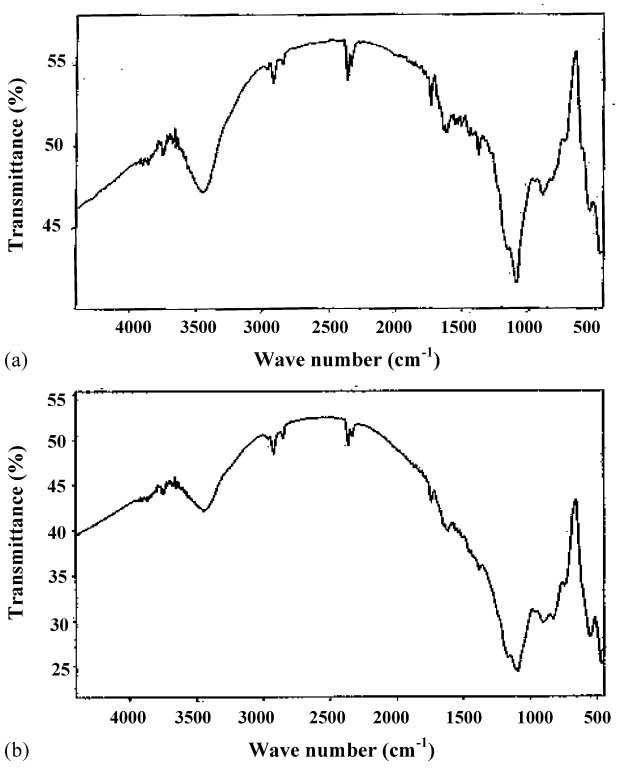

Fig. 4. FT-IR patterns of refractory materials fired at 1250 °C (a) and 1450 °C (b).

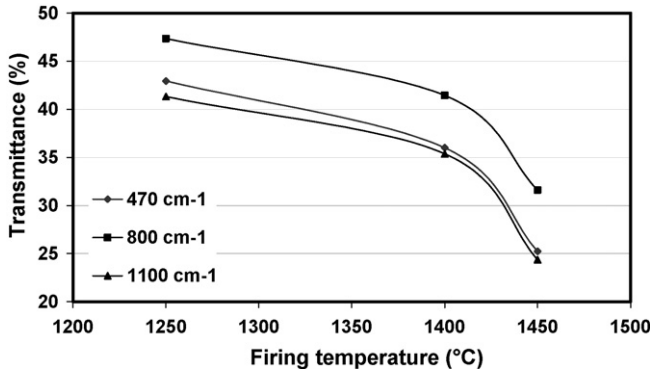

Fig. 5. Transmittance evolution of some characteristic bands of the Si–O bond in the vitreous silica vs. the firing temperature.

adsorbed water such as mentioned by Madejova [22]. Two peaks located at 1100 and 1200 cm^{-1}, characterising the mullite presence, increase as the firing temperature increases. The first peak near 1100 cm^{-1} is more important than the second. This was also observed by Suzuki et al. [28] who explain that this phenomenon is due to the specific stoichiometric composition of mullite. The temperature affects intensity of some absorption bands. Fig. 5 represents the transmittance evolution of three characteristic peaks of Si–O bond of vitreous silica at 1100, 800 and 470 cm^{-1} as a function of the firing temperature. It appears that the transmittance had undergone a systematic decrease with the temperature increase. Therefore, we can say that the amorphous phase content in the refractory samples increases.

The apparent and the absolute densities obtained, respectively, by the Archimedes's method and using helium pycnometer, for the refractory samples fired at different temperatures, are presented in Fig. 6. Absolute density of mullite obtained in this work is less than that of theoretical density of pure mullite (3.16 g/cm^3). It appears that the two densities remain nearly unchanged as the firing temperature varies. This can be explained by the fact that besides the densification, which generally appears as the temperature increases, there are transformation of cristobalite into an amorphous phase ($d = 2.5$ g/cm^3) and an increase of mullite

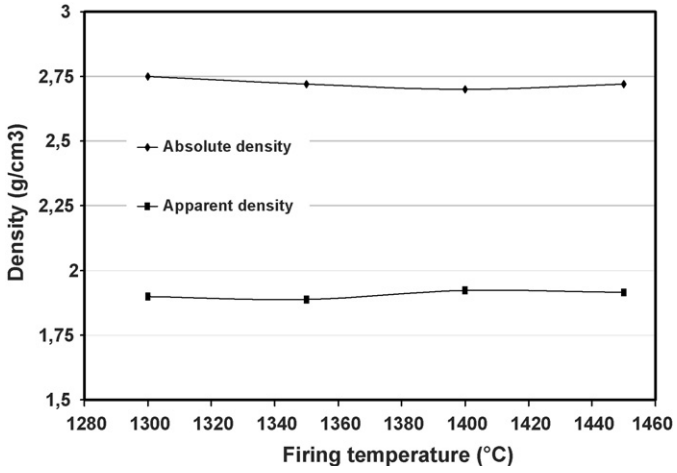

Fig. 6. Apparent and absolute density vs. firing temperature.

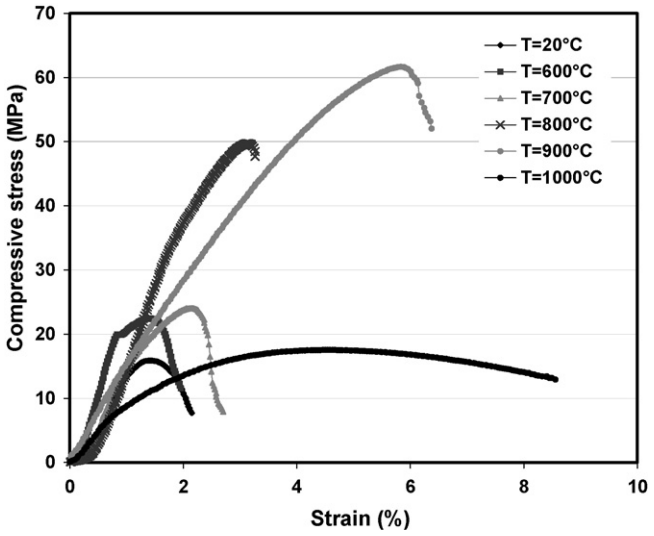

Fig. 7. Stress–strain diagrams at different test temperatures for samples fired at 1300 °C during 1 h.

content that takes place simultaneously. These would balance the supposed densification. Furthermore, we have also noticed in a previous work [8] that absolute kaolin DD3 density diminishes as the firing temperature increases beyond 1200 °C.

From the compression strength tests carried out at high temperature, we derived the stress strain diagrams for all samples. Examples of such results for samples fired at 1300 and 1400 °C are represented, respectively, in Figs. 7 and 8. The same behaviour is observed despite the differences in the stress and strain levels according to the firing temperature. The curves can be divided into three domains:

- At ambient temperature and 600 °C, the stress strain curves show a pseudo-plasticity. The strength deterioration is caused by micro-cracking and the pores interaction during loading.

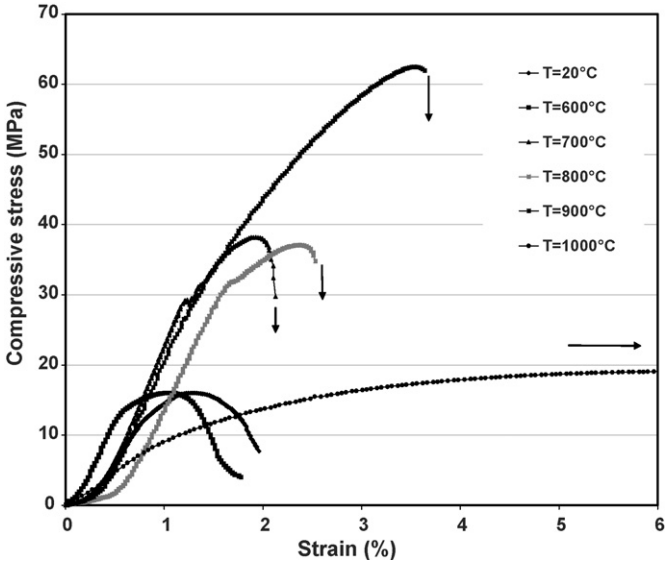

Fig. 8. Stress–strain diagrams at different test temperatures for samples fired at 1400 °C during 1 h.

- At intermediate temperatures (600–900 °C), the curves show a more important linear part. The refractory materials rigidity increases and a brittle type of failure appears. The amorphous phase viscosity was just sufficient to form bridges between different grains. This strengthening effect induces an increase of the strength by a factor 3.
- At 1000 °C, the plasticity is generalized. The samples take a rounded (barrel) form without failing. The viscosity is such that the grains can slide and accommodate as the loading increases. Creep behaviour is also possible in these conditions.

The ambient strength increases as the firing temperature increases (Fig. 9). This is related to the increase of the amorphous phase induced by the gradual transformation of the cristobalite observed when the firing temperature increases. Despite the pores density of the refractory materials, the amorphous phase seems to be beneficial at the ambient temperature. It plays the role of a vitreous binder.

The strength versus the test temperature curves for different firing temperatures are indicated in Fig. 10. These curves show three different stages. The strength is nearly constant between the ambient and 600 °C. It increases then until reaching its maximum at 900 °C beyond which it decreases sharply. This behaviour is characteristic of ceramics presenting a vitreous phase at the grains boundaries. It seems that the amorphous phase viscosity evolution with temperature governs the refractory behaviour dependence with temperature. Its transition temperature depends on its composition (silica content and the impurities of the crude kaolin). In the elastic domain for temperatures between 600 and 900 °C, the internal residual stresses relaxation increases the material strength. Beyond 900 °C, the low viscosity of the material makes it collapse easily when loaded. Even though a high strength is not really required in the general use of refractory materials, this becomes preoccupying when confronted with impacts, erosion phenomena and cyclic loading (crack initiation).

The strain corresponding to the maximal stress (strength) is as follows: from the ambient up to 600 °C, it is about 1.2% and remains constant for all firing temperatures. It then increases beyond 600 °C and depends on the firing temperature. The strain is less important for the intermediate firing temperatures (1350 and 1400 °C). The importance of the deformation for the two other extreme firing temperatures (1300 and 1450 °C) is probably due, respectively, to the bad grains cohesion and the excess of the amorphous phase.

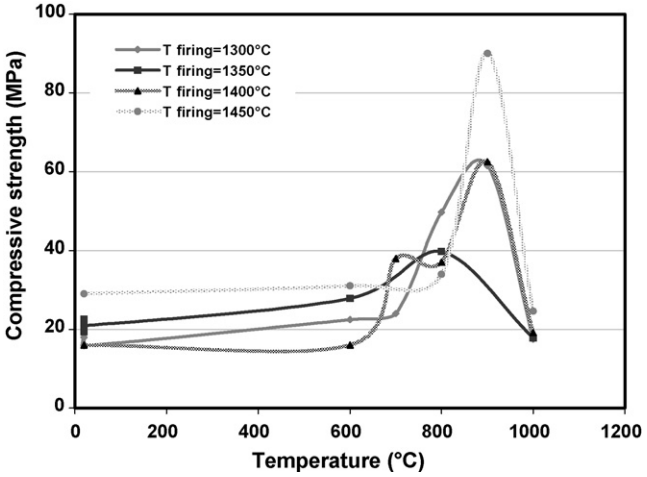

Fig. 10. Strength variation with test temperature for samples fired at different temperatures.

Fig. 11 shows the temperature dependence of Young's modulus for the different firing temperatures. The modulus values obtained are in general weak. They are appropriate for classic refractory materials presenting an important porosity. The modulus remains nearly constant until 600 °C. An earlier decrease in the modulus value is observed for the two extreme firing temperatures (1300 and 1450 °C) at around 600–700 °C whereas this variation happens at approximately 1000 °C for the intermediate firing temperatures (1350 and 1400 °C). This is directly related to the viscosity extend of the amorphous phase. The 1300 °C firing temperature does not guarantee a good cohesion of the grog grains. A firing temperature of 1450 °C is harmful because all the cristobalite is transformed into an amorphous phase.

The room temperature dynamic elastic modulus versus firing temperature shows a weak increase between 1250 and 1350 °C (Fig. 12). Above this last temperature, it undergoes a considerable augmentation. This behaviour is probably justified by the increase of the amount of the vitreous phase that permits a better rigidity at the ambient temperature.

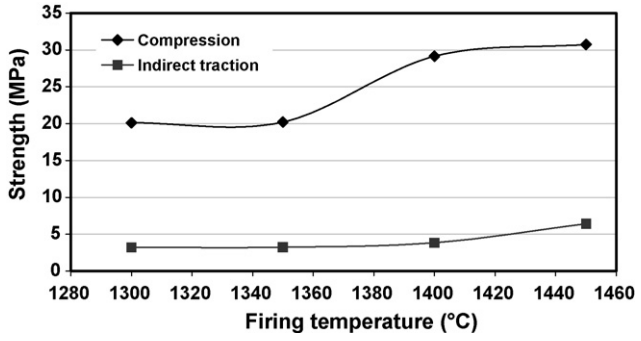

Fig. 9. Tension and compression strength (maximal stress) determined at the ambient temperature vs. firing temperature.

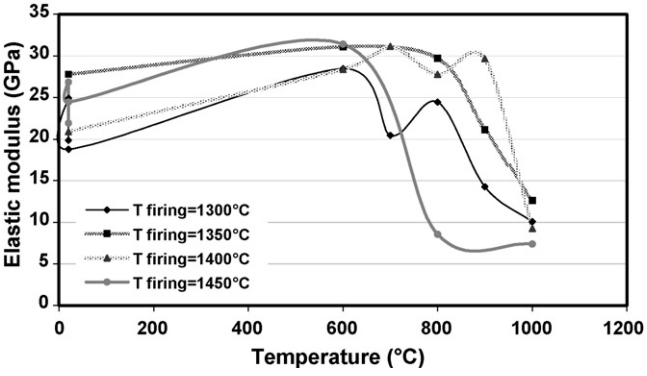

Fig. 11. Young's modulus variation with test temperature for samples fired at different temperatures.

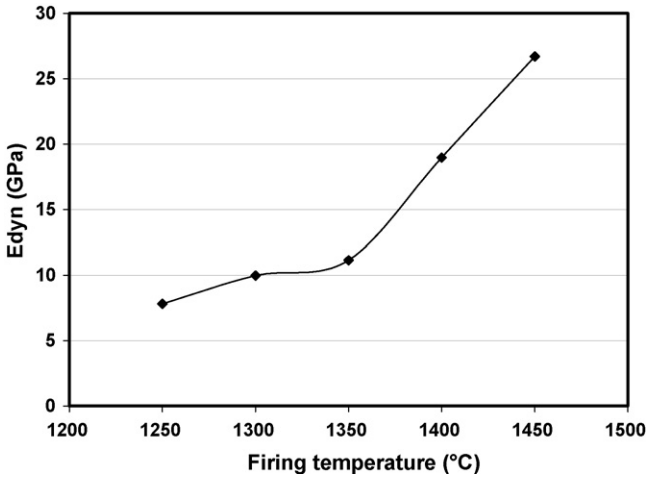

Fig. 12. Room temperature dynamic elastic modulus vs. firing temperature.

The amorphous phase dissolution kinetics enables to determine the vitreous content in the different refractory materials. The results obtained are shown in Fig. 13. We notice that the vitreous content is about 28% for the samples fired at 1300 and 1350 °C and increases up to 34% for the samples fired at 1450 °C. This evolution is directly caused by the cristobalite dissolution in the amorphous phase as the temperature increases (see Fig. 2). The chemical attack velocity is controlled by the reactions at the liquid–solid interfaces and by the powder grains microstructure. The corrosion occurs at the interconnected porosity where the vitreous phase may be present. The amorphous silica with a relatively more opened structure is more sensitive to the HF attack. Besides, the mullite can also be subject to a corrosion phenomena at a limited extend, as it is the case for other ceramics [21]. As the chemical tests were made on powders, the determined quantities include therefore the amorphous phase contained in the grog grains and at their surfaces. The thermo mechanical behaviour is controlled instead by the superficial vitreous phase or by that at the grains boundaries.

Thermal shock tests were carried out at temperatures 750, 850, 950 and 1050 °C, using a water quenching at 25 °C. The samples damage after the tests is quantified by the measure of the mechanical strength. The decrease of this strength did not

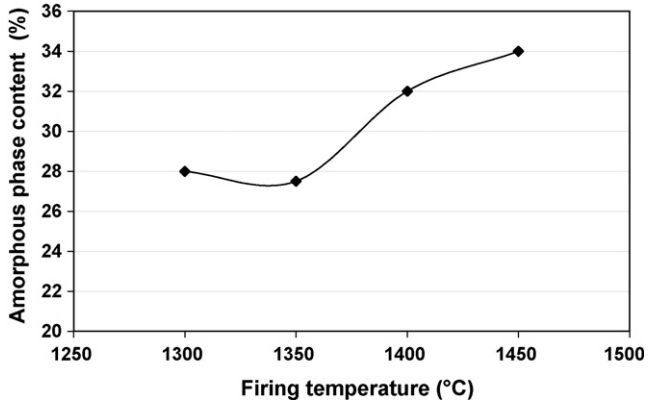

Fig. 13. Amorphous phase ratio vs. firing temperature.

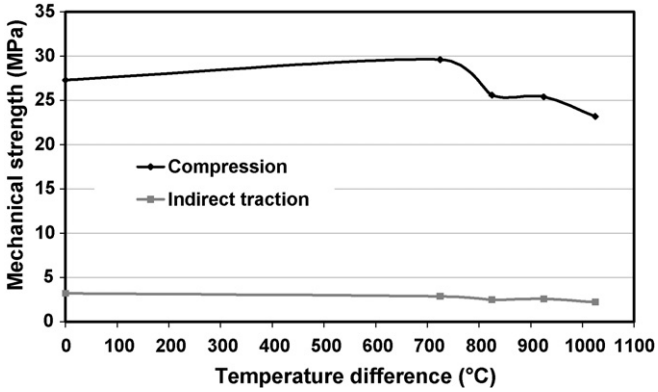

Fig. 14. Mechanical strength variation with temperature differences during thermal shock tests.

exceed 10% in all cases (Fig. 14). The thermal shock resistance of the refractory material can be explained by the effect of the amorphous phase viscosity. This behaviour is probably due to the thermal stresses relaxation induced by the structure accommodation during the early instants of the shock. A bridging effect, happened during the last moments of the thermal shock, could be another possible explanation. We also remember the fact that the mechanical strength of the samples increases in this temperature interval. This type of thermal shock behaviour is characteristic of ceramic materials containing an important amorphous phase as it is the case for zircon composites [29]. Beyond the vitreous phase transition temperature, the temperature related properties of refractory materials are directly tied to the visco-elastic behaviour of the vitreous phase.

The results of the cyclic shock, made between 950 °C and ambient temperature, are represented in Fig. 15. The samples damage occurs during the first five cycles. The mechanical loss is about 20%. After the fifth cycle, there is no appreciable mechanical strength deterioration. An example for a sample submitted to 79 thermal shock cycles is shown in Fig. 16a. We observe two types of cracking, one situated on the lateral face and the other inside the sample section. This type of cracking is caused by the sample with cylindrical form and by the kind of

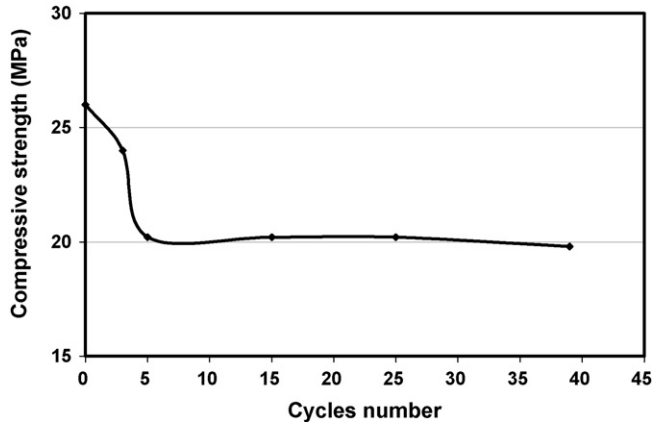

Fig. 15. Compressive strength vs. thermal shock cycles number ($\Delta T = 925$ °C) of samples fired at 1350 °C.

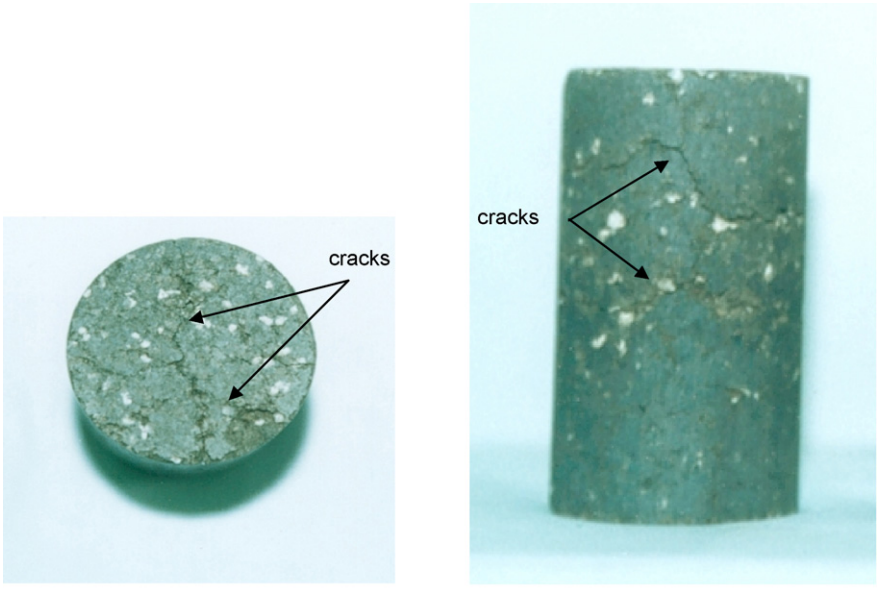

(a)

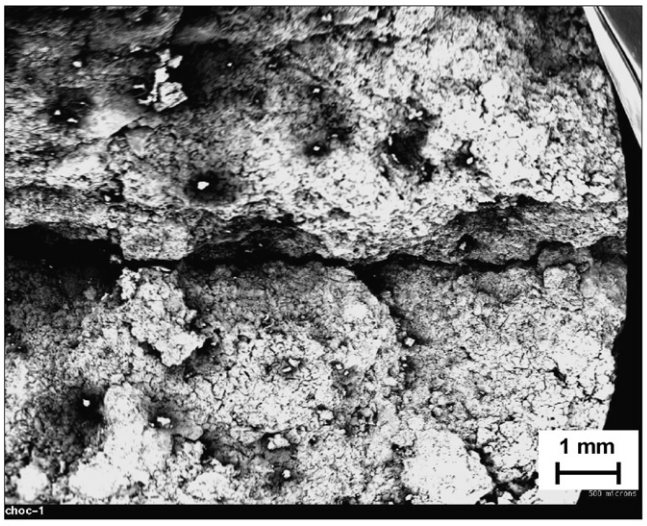

(b)

Fig. 16. Damage caused by thermal shock on the refractory samples. (a) Aspect of samples fired during 1 h at 1350 °C and having undergone 79 cycles of thermal shock with a temperature difference of 925 °C. (b) Micrograph showing cracks caused by thermal shock.

the thermal shock used (tempering in a water environment). These two facts lead to thermal stresses that act in axial and radial directions. The specific site where the crack appears on the sample faces is probably caused by a density gradient induced during processing (uniaxial pressure and sample positioning during quenching).

The average crack opening is about l00 μm (Fig. 16b). The tested samples supported 80 cycles of normalized cyclic thermal shock. Such materials are classified as good refractory materials [1].

4. Conclusion

The refractory materials made of DD3 kaolin contain mullite and rich silica amorphous phase. Silica shows two different forms: amorphous and crystalline (cristobalite). As the temperature increases, the dissolution of silica in the amorphous phase progresses, and at 1450 °C the silica is totally dissolved. The vitreous phase represents between 28% and 34% of the total product mass according to the firing temperature.

Firing temperatures of 1250 and 1300 °C are insufficient and firing at 1450 °C leads to an excess of amorphous phase. The firing temperatures between 1350 and 1400 °C generate optimal properties.

The behaviour of this refractory is governed by its amorphous phase. Indeed, the mechanical properties (at high temperature) are optimal in the interval of 600–900 °C. Beyond this interval, the plasticity is generalized. Therefore, we should limit the use of the elaborated refractory up to a temperature of 900 °C.

From the thermal shock resistance point of view, the refractory fired during 1 h at 1350 °C can be considered as a good refractory.

References

[1] G. Aliprandi, Matériaux Réfractaires et Céramiques Techniques, Septima, Paris, 1979, pp. 1–612.
[2] L.D. Pilipchatin, Sintering of Vladimirovskoe kaolin with high melting clay, Glass Ceram. 58 (1–2) (2001) 27–28.
[3] P. Lapoujade, Traité Pratique sur l'Utilisation des Produits Réfractaires, H. Vial, Paris, 1986, p. 236.
[4] M.A. Sainz, F. Serrano, J.M. Amigo, J. Bastida, A. Caballero, XRD microstructural analysis of mullites obtained from kaolinite–alumina mixtures, J. Eur. Ceram. Soc. 20 (2000) 403–412.
[5] B. Coope, An Introduction to Refractories, Raw Materials for the Refractories Industry, 2nd ed., Industrial Minerals, 1986.
[6] L. Rebouillat, M. Rigaud, Andalusite-based high-alumina castables, J. Am. Ceram. Soc. 85 (2) (2002) 373–378.
[7] H.H. Murray, Traditional and new applications for kaolin, smectite, and polygorskite: a general overview, Appl. Clay Sci. 17 (2000) 207–221.
[8] M. Gonon, G. Fantozzi, H. Osmani, M. Hamidouche, M.A. Madjoubi, K. Loucif, N. Bouaouadja, Etude de la transformation de trois nuances de kaolin en fonction de la température, Silic. Ind. 65 (11–12) (2001) 119–124.
[9] J.A. Pask, A.P. Tomsia, Formation of mullite from sol–gel mixtures and kaolinite, J. Am. Ceram. Soc. 74 (1991) 2367–2373.
[10] M. Hamidouche, N. Bouaouadja, C. Olagnon, G. Fantozzi, Thermal shock behaviour of mullite ceramic, Ceram. Int. 29 (2003) 599–609.
[11] S. Achari, L.N. Satapathy, Mullite-based refractories for molten-metal applications, Am. Ceram. Soc. Bull. 82 (3) (2003).
[12] D.M. Ibrahim, S.M. Naga, Z. Abdelkader, salamf E.A., Cordierite-mullite refractories, Ceram. Int. 21 (1995) 265–269.
[13] M.F. Zawrah, N.M. Khalil, Effect of mullite formation on properties of refractory castables, Ceram. Int. 27 (2001) 689–694.
[14] W.E. Lee, Evolution of in situ refractories in the 20th century, J. Am. Ceram. Soc. 81 (6) (1998) 1385–1410.
[15] J.S. Reed, Principles of Ceramics Processing, 2nd ed., Wiley Interscience Publication, 1995,, p. 658.
[16] P. Boch, Matériaux et processus céramiques, in: Procédés de mise en forme des céramiques, rédigé par T. Chartier, Hermes Science Publications, Paris, 2001, p. 287 (Chapitre 5).
[17] L. Saadi, E. Jabry, R. Moussa, M. Gomina, Etude des propriétés physico-chimiques et mécaniques de matériaux céramiques élaborés à partir d'une argile du Maroc: Partie I, Silic. Ind. 3–4 (1993) 51–57.
[18] M. Hamidouche, M.A. Madjoubi, K. Loucif, H. Osmani, M. Kolli, N. Bouaouadja, M. Gonon, G. Fantozzi, Processing and characterization of refractory made of Algerian kaolin, in: Proceedings of the Eighth Conference on Ceramics, INSA de Lyon, France, 3–5 September, 2002.
[19] W.O. Soboyejo, C. Mercer, J. Shymanski, S.R. Van Der Laan, Investigation of thermal shock in a high-temperature refractory ceramic: a fracture mechanics approach, J. Am. Ceram. Soc. 84 (6) (2001) 1309–1314.
[20] M. Murat, Y. Arnaud, M.El. Moussaouiti, C. Comel, Détermination des teneurs en alumino-silicates cristallisés et amorphe dans les cendres volantes et les mullites synthétiques, Silic. Ind. 6 (1984) 127–135.
[21] K.R. Mikeska, S.J. Bennison, S.L. Grise, Corrosion of ceramics in aqueous hydrofluoric acid, J. Am. Ceram. Soc. 83 (5) (2000) 1160–1164.
[22] J. Madejova, FT-IR techniques in clay mineral studies, Vib. Spectrosc. 31 (2003) 1–10.
[23] F. Farcas, P. Touze, La spectrométrie infrarouge à transformée de Fourier (IRTF), Une méthode intéressante pour la caractérisation des ciments, Bulletin des Laboratoires des Ponts et Chaussées, 230 Janvier-Février 2001, Réf. 4350, pp. 77–88.
[24] W.D. Kingery, Factors affecting thermal stress resistance of ceramic materials, J. Am. Ceram. Soc. 38 (1) (1955) 3–15.
[25] D.Ph. Hasselman, Unified theory of thermal shock fracture initiation and crack propagation in brittle ceramics, J. Am. Ceram. Soc. 52 (11) (1969) 600–604.
[26] A. Chakri, Elaboration et caractérisation des briques réfractaires de chamotte à partir des matières premières locales, Magister thesis, University of Sétif, Algeria, 1995, p. 128.
[27] Norme DIN 51 068.
[28] H. Suzuki, H. Saito, Y. Tomokiyo, Y. Soyama, Processing of ultrafine mullite powder through alkoxide route, ceramic transactions, in: S. Somiya, R.F. Davis, J.A. Pask (Eds.), Mullite and Mullite Matrix Composites, vol. 6, American Ceramic Society, Westerville, OH, 1990 , pp. 263–274.
[29] M. Hamidouche, Etude de la résistance au choc thermique, à la fatigue thermique et au fluage des céramiques à base de zircon et de mullite, Doctorat thesis, University of Setif, Algeria, 2002, p. 163.